Electronic Supplementary Information

Chemical Communications

Surface Modification Strategy for Fluorescence Solvatochromism of Carbon Dots Prepared from *p*-Phenylenediamine

Kohei Sato, Rina Sato, Yoshiki Iso* and Tetsuhiko Isobe*

Department of Applied Chemistry, Faculty of Science and Technology, Keio University, 3-14-1 Hiyoshi, Kohoku-ku, Yokohama 223-8522, Japan

*Corresponding authors.

Telephone: +81 45 566 1558 (Y.I.), +81 45 566 1554 (T.I.).

Fax: +81 45 566 1551 (T.I.).

E-mail: iso@applc.keio.ac.jp (Y.I.), isobe@applc.keio.ac.jp (T.I.).

Experimental Section

Materials

p-PD (98.0%) and DA (98.0%) were purchased from Tokyo Chemical Industry. PFDA (98.0%) was purchased from Sigma-Aldrich. Diphenyl ether (99.0%) was purchased from FUJIFILM Wako Pure Chemical. Hexane (95.0%), chloroform (99.0%), and methanol (99.8%) were purchased from Kanto Chemical. All reagents were used as received without further purification.

Preparation of CDs

p-PD (0.60 g, 5.5 mmol) was mixed with diphenyl ether (45 mL). The mixture was refluxed at 250 °C for 8 h under ambient atmosphere. After cooling to room temperature, the obtained suspension was poured into hexane (180 mL). The resulting precipitate was collected by centrifugation at ~11,000 × g (10,000 rpm, using a rotor with a diameter of 10 cm) for 10 min. After repeating the purification process three times, the precipitate was air-dried overnight to yield CD powder. The powder (1 mg) was re-dispersed in chloroform (10 mL) and methanol (10 mL) under ultrasonication. 4-Fold-diluted dispersions of these dispersions were used for characterization.

Surface modification of CDs: The as-prepared CD powder (0.10 g) was added to DA (1.59 g, 9.25 mmol). The mixture was refluxed at 170 °C for 4 h under ambient atmosphere. After cooling to room temperature, the obtained black solid was purified by redispersion in hexane (100 mL) and centrifugation at ~11,000 × g for 10 min to remove excess DA. After the purification process was repeated three times, the precipitate was air-dried overnight to yield DA-CD powder. The CD powder (0.10 g) was also added to PFDA (4.75 g, 9.25 mmol). The mixture was refluxed at 170 °C for 4 h under ambient atmosphere. After cooling to room temperature, the obtained black solid was purified by evaporating excess PFDA at 100 °C using a rotary evaporator and air-dried overnight to yield PFDA-CD powder. DA-CDs and PFDA-CD powders (1 mg) were re-dispersed in chloroform (10 mL) and methanol (10 mL) under ultrasonication. 4-Fold-diluted dispersions of these dispersions were used for characterization.

Characterization

FT-IR spectra of pressed KBr discs containing the powders were measured on an FT-IR spectrometer (JASCO, FT/IR-4200). XPS spectra were measured on an X-ray photoelectron spectrometer (JEOL, JPS-9010TR) with a Mg Kα radiation source. The binding energy of C–C/C=C bonds in the C 1s spectra at 284.4 eV was used for the

charge-up correction. The morphologies of all samples were observed with a TEM (FEI, Tecnai 12). The samples for TEM observation were prepared by drying a drop of each methanol dispersion on a copper grid covered with a carbon-reinforced collodion film (Okenshoji, COL-C10). The samples were also observed using an AFM (HITACHI, AFM5100N) in dynamic force mode. The samples for AFM were prepared by drying a drop of a methanol dispersion of each sample on a p-type silicon wafer (Nilaco, < 0.02 Ω cm). PL spectra and PLE spectra of the dispersions were measured on a fluorescence spectrometer (JASCO, FP-6500). Each spectral response was calibrated against an ethylene glycol solution of rhodamine B (5.5 g L^{-1}) and a standard light source (JASCO, ESC-333). The absolute PL QYs of the dispersions were measured on a quantum efficiency measurement system (Otsuka Electronics, QE-2000-311C). PL decay curves of the dispersions were measured on a PL lifetime spectrometer (Hamamatsu Photonics, Quantaurus-Tau C11367) equipped with 405 and 470 nm LEDs as the light sources. The PL decay curves were fitted with the following biexponential equation:

$$f(t) = A_1 exp\left(-\frac{t}{\tau_1}\right) + A_2 exp\left(-\frac{t}{\tau_2}\right), \quad (1)$$

where $f(t)$ is the PL intensity at time t, A_1 and A_2 are the amplitudes, and τ_1 and τ_2 are the PL decay times. The average PL lifetime, τ_{ave}, was calculated using equation (2).

$$\tau_{ave} = \frac{A_1{\tau_1}^2 + A_2{\tau_2}^2}{A_1\tau_1 + A_2\tau_2} \quad (2)$$

Assignments of FT-IR peaks

The FT-IR spectra of CDs, DA-CDs, PFDA-CDs, *p*-PD, DA, and PFDA are shown in Fig. S1, and assignments of the FT-IR peaks are summarized in Tables S1–S3. The CDs, DA-CDs, and PFDA-CDs maintained the structure of *p*-PD, as confirmed by the aryl C–H stretching vibrations (3060–3000 cm^{-1}; No. 9), C=C stretching vibration (1520 cm^{-1}; No. 19), C–H bending vibrations (1130–1120 cm^{-1}; No. 27, 850–830 cm^{-1}; No. 29, 520 cm^{-1}; No. 31), C=N stretching vibration (1610–1600 cm^{-1}; No. 17), and C–N stretching vibrations (1310 cm^{-1}; No. 24, 1270–1250 cm^{-1}; No. 25).

The CDs retained the amino group in *p*-PD, as confirmed by the NH_2 asymmetric and symmetric stretching vibrations (3420–3360 cm^{-1}; No. 2, 3320 cm^{-1}; No. 3), overtone of NH_2 bending vibration (3200 cm^{-1}; No. 4), and NH_2 bending vibrations (1630 cm^{-1}; No. 16, 770–650 cm^{-1}; No. 30). In contrast, the DA-CDs contained amide bonds rather than amino groups, as confirmed by the N–H stretching vibration (3320 cm^{-1}; No. 7), overtone of CNH bending and C–N stretching vibrations (3150 cm^{-1}; No. 8), C=O stretching vibration (1650 cm^{-1}; No. 15), and CNH bending and C–N stretching vibrations (1550 cm^{-1}; No. 18). Furthermore, the DA-CDs contained alkyl chains, as verified by the CH_3 asymmetric and symmetric stretching vibrations (2960 cm^{-1}; No. 10, 2870 cm^{-1}; No. 12), CH_2 asymmetric and symmetric stretching vibrations (2920 cm^{-1}; No. 11, 2850 cm^{-1}; No.

13), CH_2 and CH_3 asymmetric bending vibrations (1470 cm^{-1}; No. 21), and CH_3 symmetric bending vibration (1410 cm^{-1}; No. 23), which were not detected for the CDs. The DA-CDs did not have carboxy groups because there were no signals due to the O–H stretching vibrations (3400–3000 cm^{-1}; No. 6) or C–OH bending vibration (1430 cm^{-1}; No. 22), which were observed for DA. This finding reveals that the CDs are modified with DA through amide bonds to form DA-CDs, as already shown in Fig. 1. In addition, the peak assigned to the C=O stretching vibration for DA-CDs (1650 cm^{-1}; No. 15) was located at a lower wavenumber than that for DA (1700 cm^{-1}; No. 14), which is attributed to the weakened bond strength of C=O caused by electron donation from nitrogen to carbon in the amide bond due to the resonance effect for DA-CDs.[S1]

The PFDA-CDs also contained amide bonds rather than amino groups, as confirmed by the N–H stretching vibration (3330 cm^{-1}; No. 7), overtone of CNH bending and C–N stretching vibrations (3160 cm^{-1}; No. 8), C=O stretching vibration (1700 cm^{-1}; No. 15), and CNH bending and C–N stretching vibrations (1560 cm^{-1}; No. 18). Furthermore, the PFDA-CDs contained perfluoroalkyl chains, as verified by the C–F stretching vibrations (1350–1100 cm^{-1}; No. 28), which were not detected for the CDs. The PFDA-CDs did not contain carboxy groups because there were no signals due to O–H stretching vibrations (3600–3400 cm^{-1}; No. 5) or C–OH bending vibration (1460 cm^{-1}; No. 22), which were

observed for PFDA. This result reveals that the CDs were modified with PFDA through amide bonds to form PFDA-CDs, as already shown in Fig. 1. In addition, the peak assigned to the C=O stretching vibration for PFDA-CDs (1700 cm^{-1}; No. 15) was located at the same wavenumber as that for PFDA (1700 cm^{-1}; No. 14), which is attributed to two opposite two factors: electron donation from nitrogen in the amide bond by the resonance effect and electron withdrawal from the perfluoroalkyl group by the inductive effect.

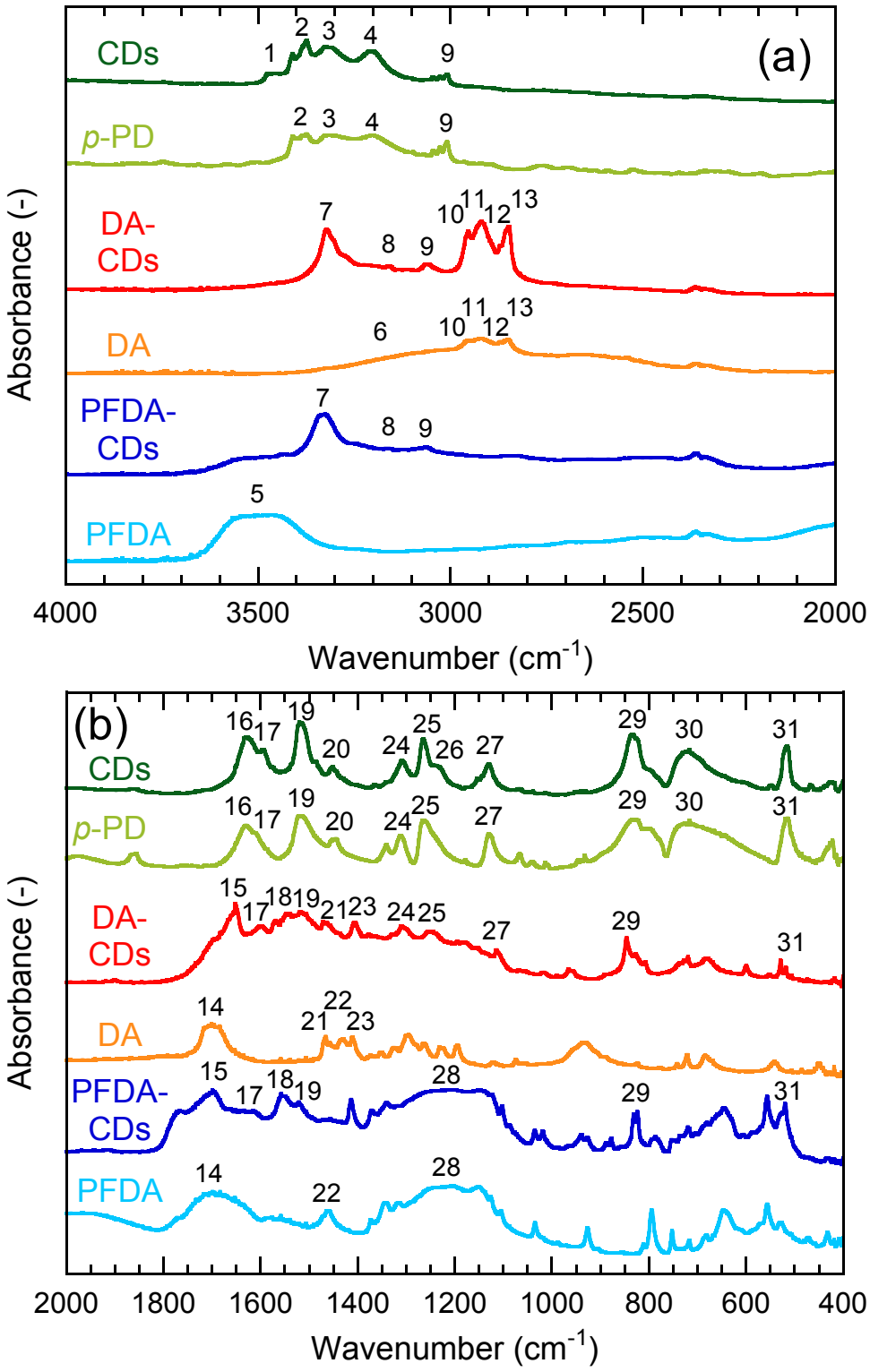

Figure S1. FT-IR spectra of the CDs, *p*-PD, DA-CDs, DA, PFDA-CDs, and PFDA in the ranges of (a) 4000–2000 cm^{-1} and (b) 2000–400 cm^{-1}.

Table S1. Assignments of FT-IR peaks of CDs and *p*-PD.

Peak number	Peak position (cm^{-1})		Assignment[S1]
	CDs	*p*-PD	
1	3480–3420		N–H stretching
2	3420–3360	3420–3360	NH_2 asymmetric stretching
3	3320	3330	NH_2 symmetric stretching
4	3200	3200	overtone of NH_2 bending
9	3050–3000	3050–3000	aryl C–H stretching
16	1630	1630	NH_2 bending
17	1600	1610	C=N stretching
19	1520	1520	aryl ring semicircle stretching
20	1450	1450	aryl ring semicircle stretching
24	1310	1310	aryl C–N stretching
25	1270	1270	aryl C–N stretching
26	1230		aryl C–O stretching
27	1130	1130	in-plane bending
29	840	830	H wagging
30	770–650	770–650	NH_2 wagging
31	520	520	out-of-plane bending

Table S2. Assignments of FT-IR peaks of DA-CDs and DA.

Peak number	Peak position (cm^{-1})		Assignment[S1]
	DA-CDs	DA	
6		3400–3000	O–H stretching
7	3320		NH stretching
8	3150		overtone of CNH bending overtone of C–N stretching
9	3060		aryl C–H stretching
10	2960	2960	CH_3 asymmetric stretching
11	2920	2920	CH_2 asymmetric stretching
12	2870	2870	CH_3 symmetric stretching
13	2850	2850	CH_2 symmetric stretching
14		1700	C=O asymmetric stretching
15	1650		C=O stretching
17	1600		C=N stretching
18	1550		CNH bending C–N stretching
19	1520		aryl ring semicircle stretching
21	1470	1470	CH_2 bending CH_3 asymmetric bending
22		1430	C–OH bending
23	1410	1410	CH_3 symmetric bending
24	1310		aryl C–N stretching
25	1250		aryl C–N stretching
27	1120		in-plane bending
29	850		H wagging
31	520		out-of-plane bending

Table S3. Assignments of FT-IR peaks of PFDA-CDs and PFDA.

Peak number	Peak position (cm^{-1})		Assignment[S1]
	PFDA-CDs	PFDA	
5		3600–3400	O–H stretching
7	3330		NH stretching
8	3160		overtone of CNH bending overtone of C–N stretching
9	3060		aryl C–H stretching
14		1700	C=O asymmetric stretching
15	1700		C=O stretching
17	1610		C=N stretching
18	1560		CNH bending C–N stretching
19	1520		aryl ring semicircle stretching
22		1460	C–OH bending
28	1350–1100	1350–1100	C–F stretching
29	830		H wagging
31	520		out-of-plane bending

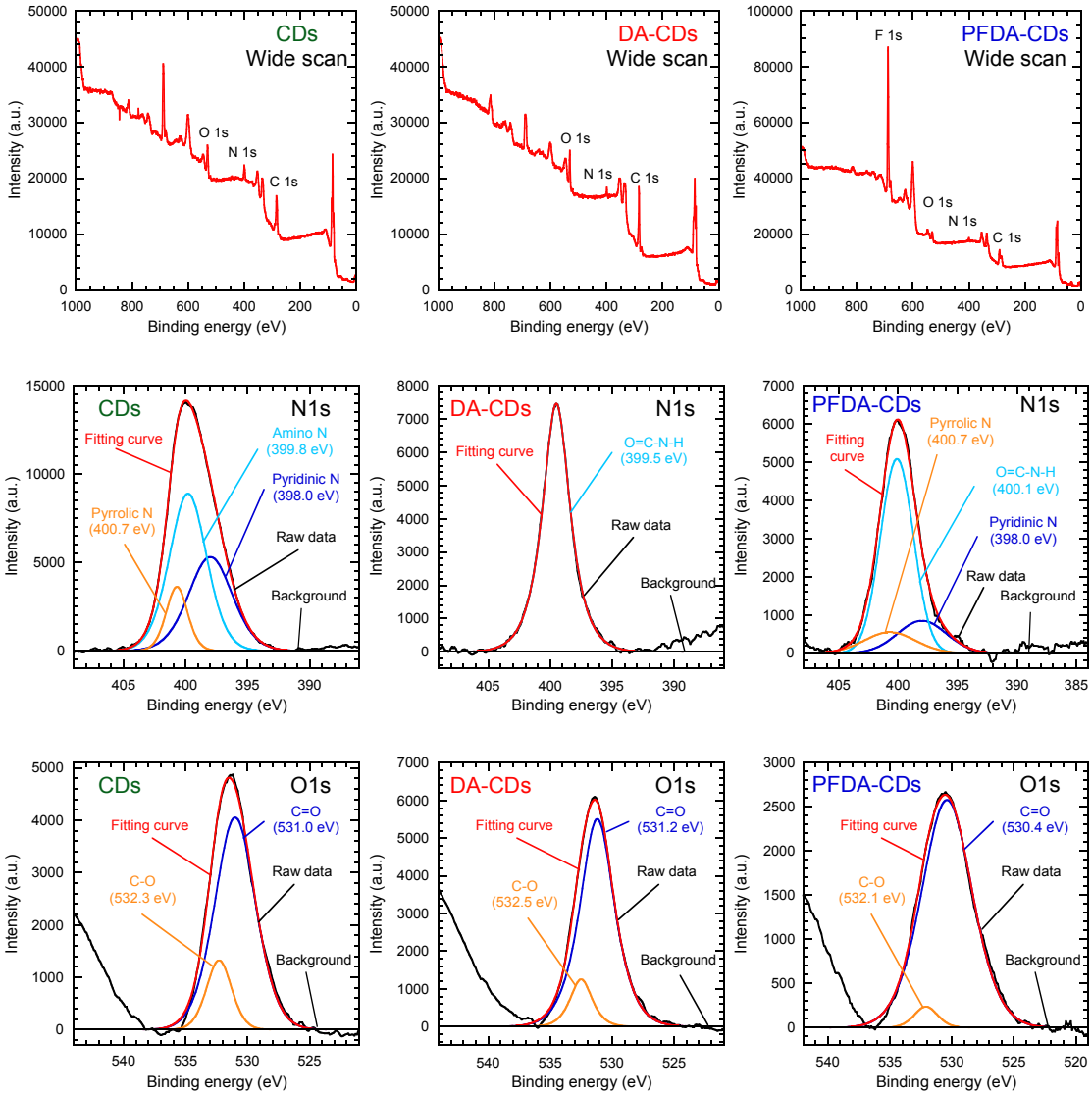

Figure S2. Wide-scan, N 1s, and O 1s XPS spectra of CDs, DA-CDs, and PFDA-CDs.

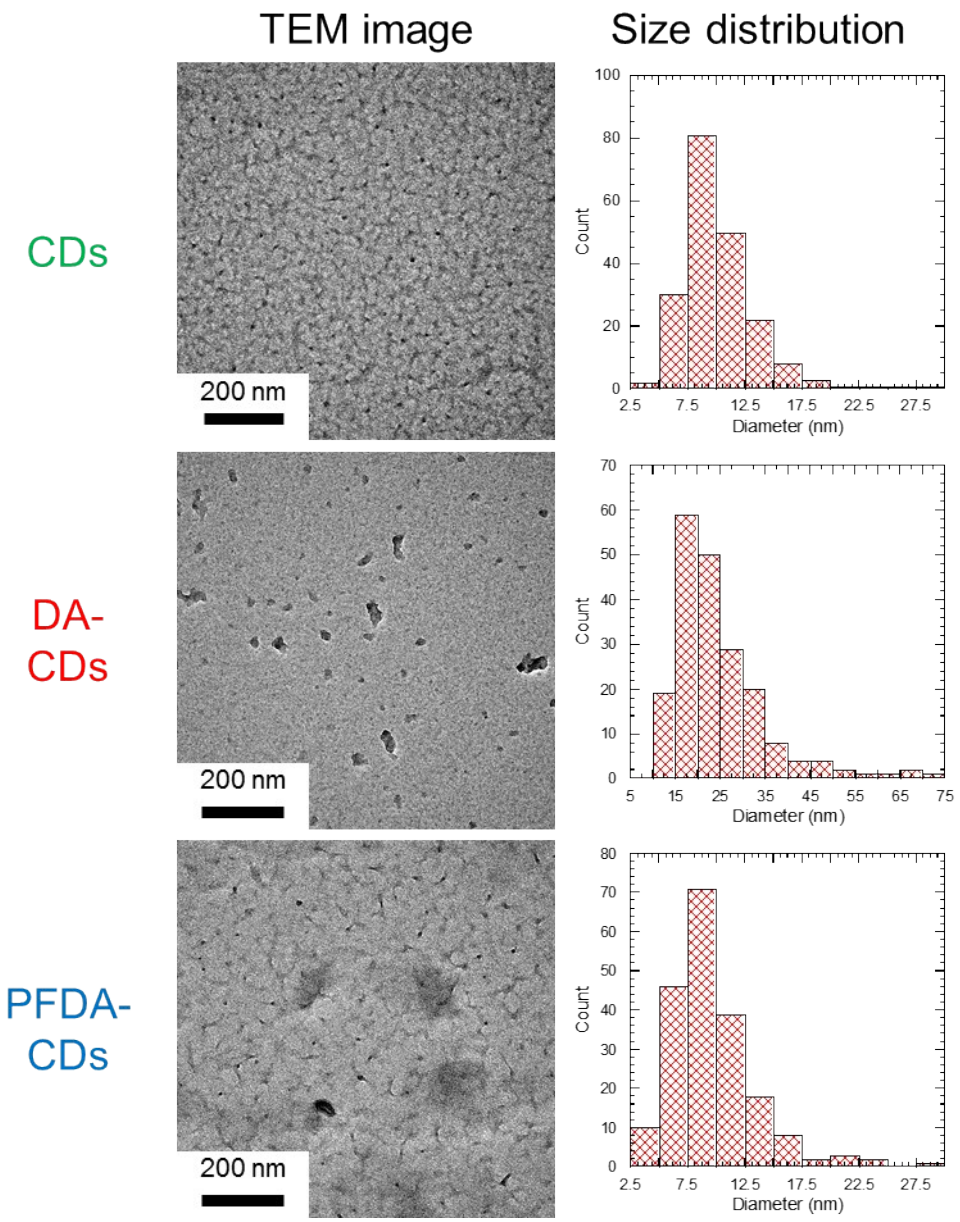

Figure S3. TEM images and particle size distributions of the CDs, DA-CDs, and PFDA-CDs.

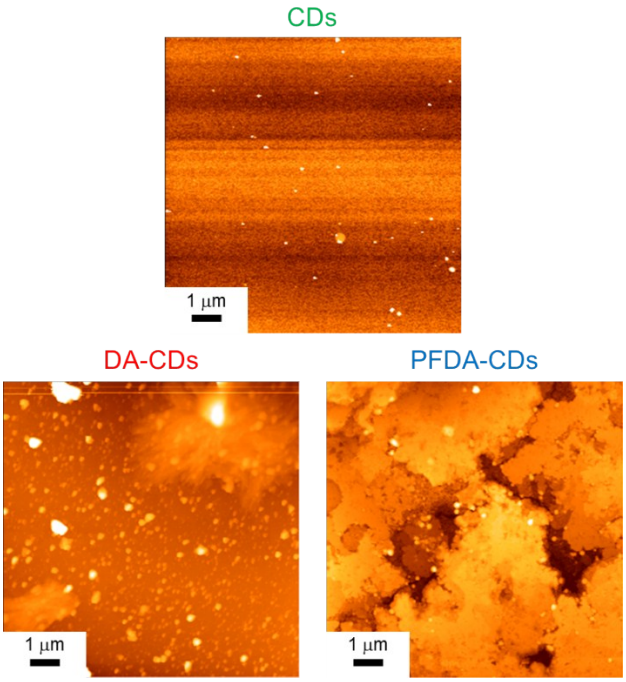

Figure S4. AFM images of the CDs, DA-CDs, and PFDA-CDs.

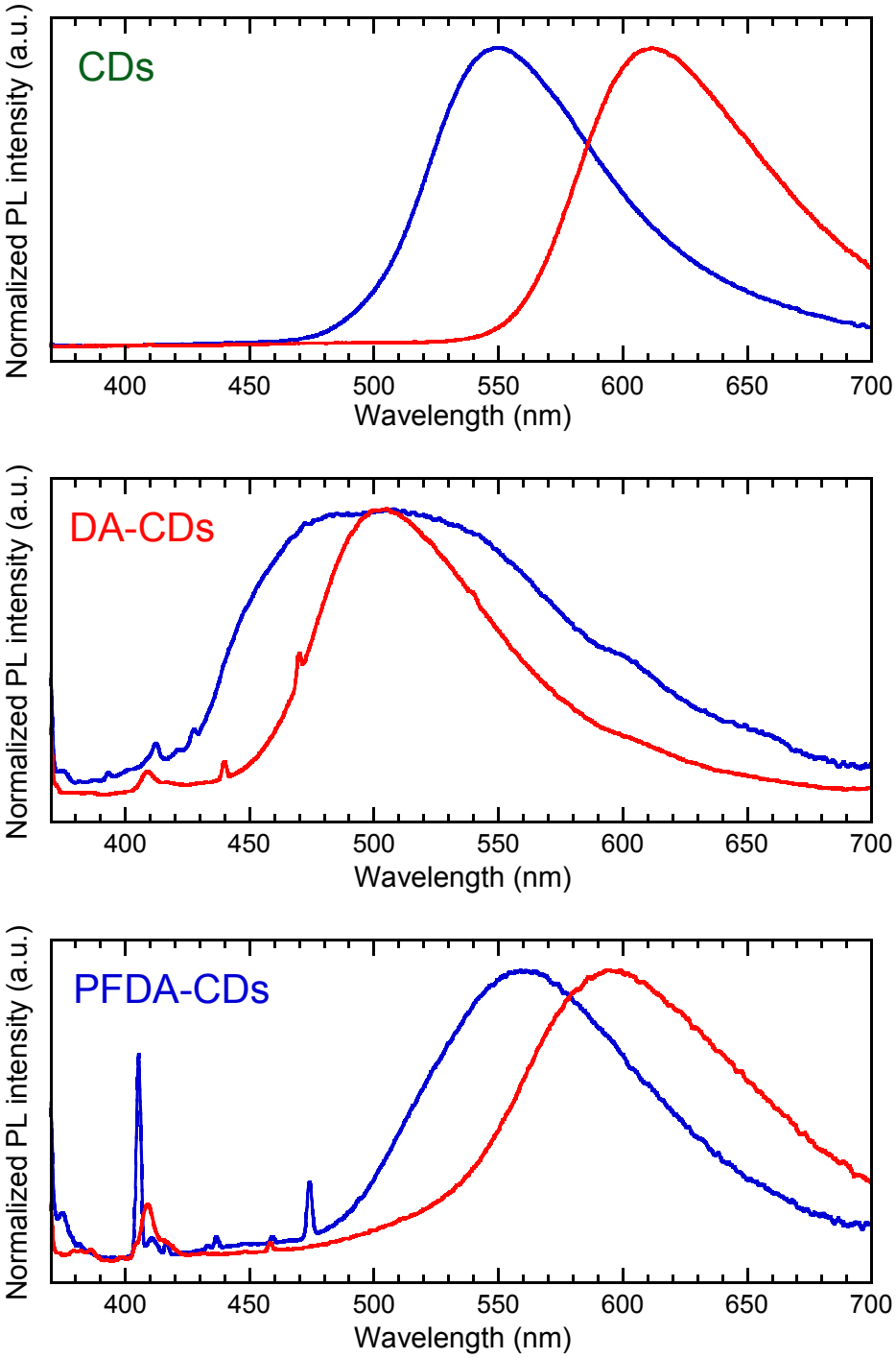

Figures S5. Normalized PL spectra of CDs, DA-CDs, and PFDA-CDs in chloroform (blue) and methanol (red) under 365 nm excitation.

Table S4. PL/PLE peak wavelengths and PL full widths at half maximum (FWHMs) of chloroform and methanol dispersions of each sample and PL/PLE peak shifts between both dispersions.

Sample	Chloroform			Methanol			Peak Shift	
	λ_{ex} (nm)	λ_{em} (nm)	FWHM (nm)	λ_{ex} (nm)	λ_{em} (nm)	FWHM (nm)	$\Delta\lambda_{ex}$ (nm)	$\Delta\lambda_{em}$ (nm)
CDs	473	556	84	517	611	90	44	55
DA-CDs	418	501	142	424	504	83	6	3
PFDA-CDs	455	561	103	533	598	104	78	37

Table S5. Absolute PL QYs of chloroform and methanol dispersions of each sample excited at the optimum excitation wavelength.

Sample	Chloroform		Methanol	
	λ_{ex} (nm)	PL QY (%)	λ_{ex} (nm)	PL QY (%)
CDs	473	30.3	517	14.1
DA-CDs	418	0.244	424	1.59
PFDA-CDs	455	4.19	533	0.861

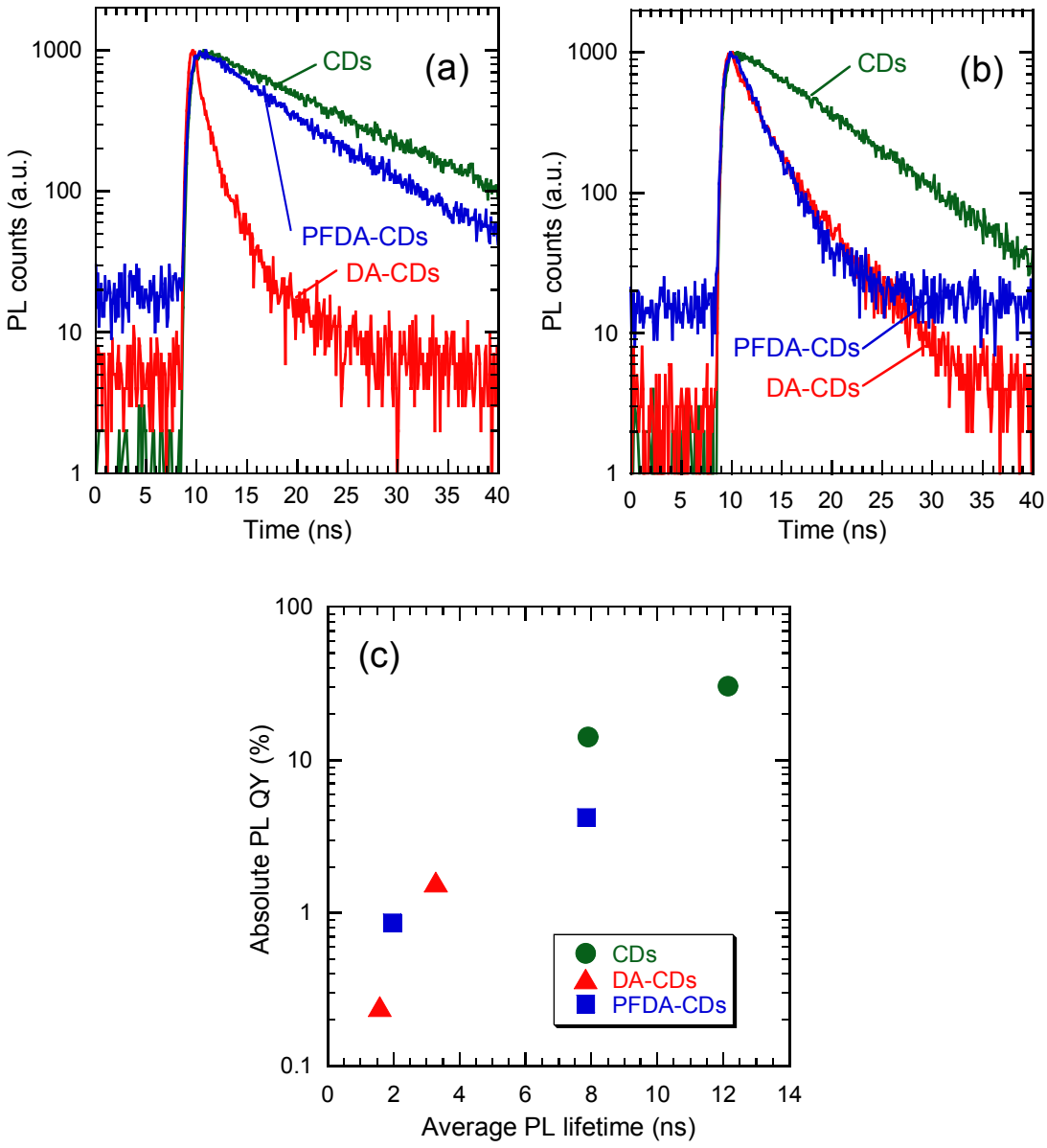

Figures S6. (a, b) PL decay curves of CDs, DA-CDs, and PFDA-CDs in (a) chloroform and (b) methanol. λ_{ex}: 405 nm (DA-CDs) and 470 nm (CDs, PFDA-CDs). (c) Correlation between the average PL lifetime and the absolute PL QY.

Table S6. Fitted parameters of the PL decay curves of chloroform and methanol dispersions of each sample.

Solvent	Sample	τ_1 (ns)	A_1 (%)	τ_2 (ns)	A_2 (%)	τ_{ave} (ns)	χ^2
Chloroform	CDs	2.76	29.1	13.1	70.9	12.3	0.988
	DA-CDs	0.556	80.3	2.45	19.7	1.54	1.45
	PFDA-CDs	2.28	39.7	8.93	60.3	7.97	1.05
Methanol	CDs	0.572	35.8	7.97	64.2	7.68	1.02
	DA-CDs	1.61	61.0	4.46	39.0	3.43	0.899
	PFDA-CDs	1.14	58.4	2.51	41.6	1.98	1.18

References

S1 P. J. Larkin, *Infrared and Raman Spectroscopy: Principles and Spectral Interpretation*, *2nd ed.*, ELSEVIER, Amsterdam, 2018.